SAND2019-8335C

A Direct Comparison of Transverse Velocimetry Techniques Using Photon Doppler Velocimetry (PDV) in Oblique Impact Experiments

Christopher R. Johnson[1, a)] John P. Borg[1, b)] and C. Scott Alexander[2]

[1] *Marquette University, Department of Mechanical Engineering, Milwaukee, Wisconsin 53233*
[2]*Sandia National Laboratories, Albuquerque, New Mexico*

[a)] christopher.r.johnson@marquette.edu
[b)] john.borg@marquette.edu

Abstract. Photon Doppler velocimetry has been used increasingly to measure transverse velocity in dynamic experiments. This work presents an oblique impact experiment which was performed using a slotted-barrel gas gun to generate normal and shear stress waves resulting in longitudinal and transverse velocity. Multiple transverse PDV configurations were implemented and directly compared. Results illustrate variability between the velocimetry methods, aiming to further advance transverse velocimetry measurements.

INTRODUCTION

Development and implementation of photon Doppler velocimetry (PDV) in dynamic compression testing has enabled high temporal resolution velocimetry measurements in many experimental studies [1], [2]. Many dynamic compression experiments are primarily uniaxial, where an optical probe is oriented normal to a surface to measure longitudinal velocity and equated to stress. Additional techniques aim to characterize complex loading states which requires an additional measurement of transverse velocity to quantify shear stress. This has spawned many efforts to employ PDV for transverse velocimetry and is the primary interest of this work.

Multiple groups have developed techniques for measuring transverse velocity. Early developments can be traced to Clifton's group at Brown University, where they developed a transverse displacement interferometer (TDI) using VISAR (Velocity Interferometer System for Any Reflector) [3], [4]. The advent of PDV has allowed similar pursuits through fiber optic arrangements. Many techniques can be found in the literature which measure transverse velocity using PDV, however, no direct comparison of these methods exist. This work aims to directly compare techniques in a controlled experiment and identify strengths and weaknesses within the methodologies.

THEORY

Oblique impact gas-gun experiments are used as a technique to quantify deviatoric behavior of materials. To perform these experiments, a projectile with an angled flyer plate impacts a target at an identical inclination (Fig. 1). Because of the nature of the experiment, longitudinal and shear stress waves are imparted. The stress states result in longitudinal and transverse wave velocities and quantify deviatoric behavior of materials. Further description of this experiment can be found in various works [5]–[17].

To perform these experiments, fiber optic probes (collimators, focusing probes, etc.) are placed on the downrange side of a target as in Fig. 1. Optical paths are incident on the rear surface of the target and observe a Doppler shift in frequency indicative of a surface velocity. Equation 1 summarizes this relationship, where f_b is the

Sandia National Laboratories is a multimission laboratory managed and operated by National Technology & Engineering Solutions of Sandia, LLC, a wholly owned subsidiary of Honeywell International Inc., for the U.S. Department of Energy's National Nuclear Security Administration under contract DE-NA0003525.

beat frequency, f_0 is the carrier frequency, V^* is the apparent velocity, and λ_{Laser} is the wavelength of the incident target laser. Various forms and notation of this equation may be seen across literature.

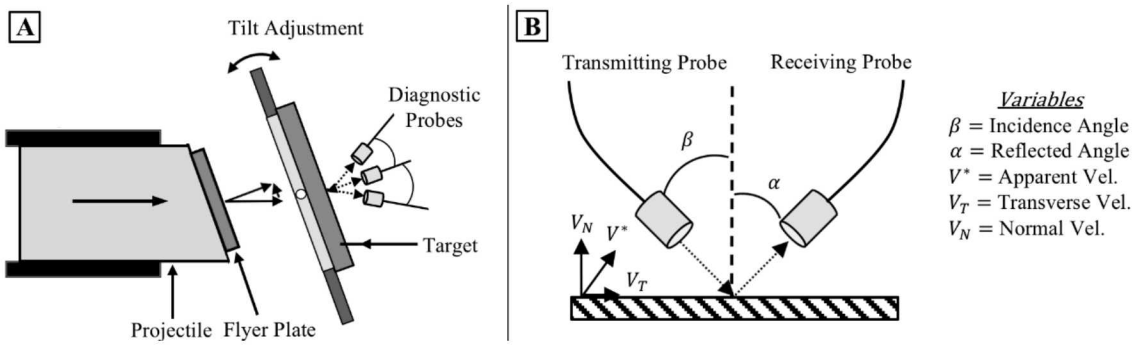

FIGURE 1. (A) Oblique impact configuration. A projectile with a flyer plate impacts a target with incident diagnostic probes. (B) General nomenclature used for denoting the optical paths for transmitted and reflected light.

$$V^* = \frac{1}{2}(f_b - f_0)\lambda_{Laser} \tag{1}$$

Apparent velocity, V^*, is used to denote the velocity observed along the optical path of the incident and reflected light. The general form of the equation can be seen in Eq. 2, where V_N indicates normal surface velocity, V_T denotes transverse velocity, V_E signifies the out of plane component of velocity, β symbolizes the angle of the transmitted optical path, α indicates the reflected optical path angle, and γ and φ denote the out of plane angles. Proper orientation of the optical package allows for variables V_E, γ and φ to be neglected. Because of the various ways to make interferometry measurements, different expressions can be formulated using Eq. 2. The following section will detail three configurations which leverage this equation.

$$V^* = \frac{V_N}{2}(\cos\alpha + cos\beta) + \frac{V_T}{2}(\sin\alpha + sin\beta) + \frac{V_E}{2}(\sin(\gamma) + \sin(\varphi)) \tag{2}$$

SYSTEMS

The following details the three systems integrated into this study. They will be referenced by the following names: *AO device*, *traditional heterodyne*, and *frequency multiplexed heterodyne*. Recall each system allows for measurement of transverse velocity.

Zuannetti *et al.* [18] and Kettenbiel *et al.* [19] have detailed PDV arrangements which optically combine two off-axis probes at symmetric inclination angles about a surface normal. This approach is elegant and observes only the transverse component of velocity (Fig. 2A). Mathematically, this system is described by Eq. 3, and is simplified to Eq. 4 due to geometric symmetry of the optical paths. Variables in Eq. 3 denote the differential between the two apparent velocities observed V_1^* and V_2^*, the surface velocities V_N and V_T, and the corresponding optical paths for the system α_1, β_1, α_2, and β_2. The significant benefit to this approach is the system's insensitivity to longitudinal velocity. A downside is limited temporal resolution. To remedy this issue, Kettenbiel *et al.* implemented an acousto-optic frequency modulator on one optical leg of the interferometer, hence the systematic name *AO device*. The ingenuity increases the carrier frequency in the signal and increased the temporal resolution of the signal.

$$V^* = V_2^* - V_1^* = \frac{V_N}{2}(\cos\alpha_2 + cos\beta_2 - \cos\alpha_1 - cos\beta_1) + \frac{V_T}{2}(\sin\alpha_2 + sin\beta_2 - \sin\alpha_1 - sin\beta_1) \tag{3}$$

$$V_T = \frac{2V^*}{sin\alpha_2 - sin\alpha_1} = \frac{V^*}{sin\alpha} \tag{4}$$

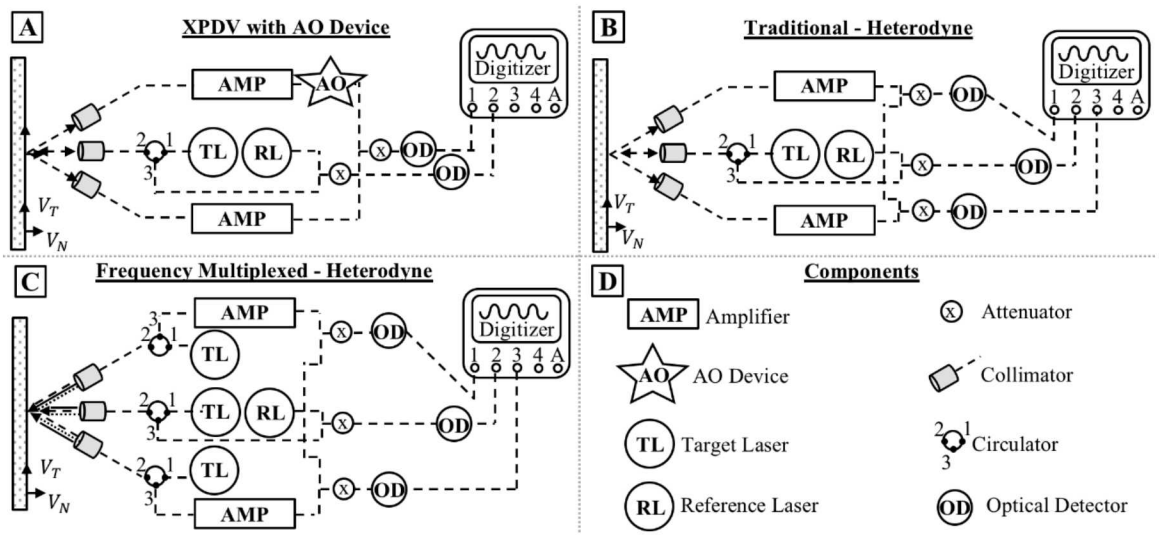

FIGURE 2. Schematic of the three PDV configurations tested in this work. (A) Illustrates the AO Device setup. (B) Features a traditional heterodyne system. (C) Displays the frequency multiplexed heterodyne system. (D) Depicts components.

Traditional heterodyne systems function by upshifting the differential beat frequency (Fig. 2B). This approach has been widely described by many [1], [2], [20]–[22], and allows for high temporal resolution in a signal. Using Eq. 2, this technique allows for the transverse velocity to be mathematically determined by measuring a longitudinal velocity and apparent velocity. Equation 5 defines this expression, where the subscript, *'i'* denotes the number of apparent velocity measurements made. Systematic benefits are high temporal resolution and convenience of using a conventional system, while the downsides resonate in the magnitude difference between the longitudinal and transverse velocities and limited number of measurements. In this case, the quantity of transverse measurements is governed by the amount off-axis probes. Therefore, only two transverse measurements are made with this method.

$$V_{T_i} = \frac{2(V_i^*) - V_N(cos\alpha_i + cos\beta_i)}{sin\alpha_i + sin\beta_i} \tag{5}$$

The multiplexed frequency heterodyne system is an extension of the traditional heterodyne approach, and functions by using three individual lasers to transmit three distinct wavelengths. This approach has been discussed by Daykin, Moro, and Danielson [23]–[25] for various longitudinal velocity measurements, however, no works display this implementation for transverse velocity measurements. Logistics of this configuration are illustrated in Fig. 2C, where three lasers with distinct wavelengths scatter light along the optical paths of the three probes. The reference laser is then tuned such that the three distinct beat frequencies are within the bandwidth of the oscilloscope and optical detectors. Nine unique velocity measurements with different components of normal and transverse velocity are resolved. Akin to the AO device and traditional heterodyne approaches, Eq. 3 and 5 can be used to describe this system. Although many permutations of Eq. 3 and Eq. 5 exist, only Eq. 5 will be used to calculate six transverse velocity profiles. Like the traditional heterodyne system, this approach enables high temporal resolution, the convenience of using a conventional system, and eliminates systematic cross-talk because of three distinct wavelengths. Additionally, redundancy in measurements allow for statistical approaches to be applied to the data. Disadvantages still manifest in the magnitude difference between the longitudinal and transverse velocities.

PROPAGTAION OF UNCERTAINTIES

Uncertainty of transverse velocity measurements are determined by propagating the uncertainty of independent variables. The general expressions can be seen in Eq. 6 and 7. Note again the subscript, *i*, defines the multiple measurements which can be obtained. Considering that two and six transverse profiles are acquired for the

traditional heterodyne and multiplexed approaches, a weighted averaging scheme is applied. Relations 8, 9, and 10 describe the scheme, where w_i denotes the weighted scheme.

XPDV: $$\delta V_T = \sqrt{\left[\frac{\partial V_T}{\partial \mathrm{V}^*}\delta V^*\right]^2 + \left[\frac{\partial V_T}{\partial \mathrm{V_N}}\delta V_N^2\right]^2 + \left[\frac{\partial V_T}{\partial \alpha_1}\delta\alpha_1\right]^2 + \left[\frac{\partial V_T}{\partial \alpha_2}\delta\alpha_2\right]^2 + \left[\frac{\partial V_T}{\partial \beta_1}\delta\beta_1\right]^2 + \left[\frac{\partial V_T}{\partial \beta_2}\delta\beta_2\right]^2} \quad (6)$$

Heterodyne Systems: $$\delta V_{T_i} = \sqrt{\left[\frac{\partial V_T}{\partial \vec{V}^*}\delta V^*\right]^2 + \left[\frac{\partial V_T}{\partial \vec{V}_N}\delta V_N^2\right]^2 + \left[\frac{\partial V_T}{\partial \alpha_i}\delta\alpha_i\right]^2 + \left[\frac{\partial V_T}{\partial \beta_i}\delta\beta_i\right]^2} \quad (7)$$

$$\bar{V}_T = \frac{\sum_{i=1}^{N} w_i V_{T_i}}{\sum_{i=1}^{N} w_i} \quad (8) \qquad w_i = \left(\frac{1}{\delta V_{T_i}}\right)^2 \quad (9) \qquad \delta\bar{V}_T = \left(\sum_{i=1}^{N} w_i\right)^{-\frac{1}{2}} \quad (10)$$

METHODS

Experiments were performed on Sandia National Laboratory's 100-millimeter oblique light gas-gun. The impactor and target used were composed of Ti-6Al-4V, Diameters of the impactor and target were 76.24 millimeters with thicknesses of 7.97 mm and 4.00 millimeters. Skew angle of the impactor, θ, was 15 degrees. Acoustic wave speeds for the longitudinal velocity, C_L, and shear velocity, C_S were assumed to be 6.12 km/s and 3.17 km/s [9].

PDV configurations implemented are the three systems mentioned in this work. AC Photonic collimators with a 70mm working distance were used. Inclination of the off-axis collimators relative to the surface normal were $\alpha = -20°, +20°$. An uncertainty of $\pm 1°$ was assumed for the probe angles. The carrier frequency of the AO system was 0.2 GHz, 3 GHz for the traditional heterodyne, and 3, 5, and 7 GHz for the frequency multiplexed signals.

RESULTS & DISCUSSION

Reduction of PDV signals were performed using Sandia's data reduction tool SIRHEN [26], a part of the SMASH [27] software package. For the AO signal, duration of each STFT window (τ) was 2.799e-7s with an overlap of 6. Heterodyne signals were processed with a duration window of 9.322e-8s and an overlap of 6. Resulting spectrograms are illustrated in Fig. 3. It should be noted that the AO signal had a lower signal to noise ratio when compared to the heterodyne traces due to the carrier frequency of the system. Velocity uncertainties were quantified using the approach describe in Dolan's work [28].

Figure 4 illustrates the transverse velocity profiles. Vertical black dashed lines are implemented to depict expected arrival times of the two waves, as well as the expected shear window. Longitudinal velocities are illustrated for both heterodyne signals in the red and blue dashed lines, and the transverse velocities are displayed by the continuous lines with uncertainty bands. Arrival time of the waves agree with the longitudinal and transverse signal. Both longitudinal and transverse velocities have high magnitude correlation. A slight deviation can be noticed in the rise of the multiplexed transverse signal when compared with the AO device and traditional heterodyne signals. This can likely be attributed to the experimental setup. Optical wiring of the system allowed for the AO device and traditional heterodyne system to be incident on the same point on the rear surface, while the multiplexed signal was positioned on a different point.

Analysis of Fig. 4 also illustrates uncertainty variability between systems. It is apparent that the traditional heterodyne system has larger measurement uncertainty, and the signal is quite noisy. Comparison of the AO device and multiplexed system reveal slightly lower uncertainty in the multiplexed measurements, where the main difference lies in the temporal resolution attained with the multiplexed system. Additionally, the multiplexed system measured the expected magnitude of transverse velocity with slightly higher accuracy than the AO technique.

CONCLUSION

A direct comparison between transverse velocimetry techniques was performed. The three systems illustrate methods which can be used to quantify transverse velocity. Measurements of velocities appear to be of similar magnitudes, however, uncertainties appear to differ. The analysis performed using the traditional and multiplexed system appear to have slight noise, while the AO device has significant temporal limitations. Uncertainties for the

AO Device and traditional system are of similar magnitudes, while the multiplexed approach has reduced uncertainty. Depending on systematic requirements, either the AO or multiplexed techniques may suffice.

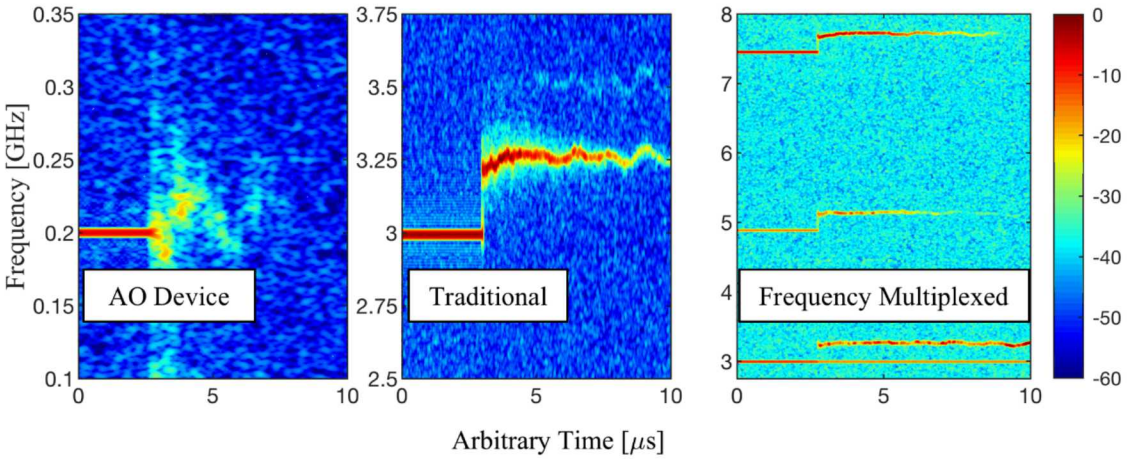

FIGURE 3: Spectrograms from the various systems. (A) The AO system. (B) Traditional heterodyne system. (C) Frequency multiplexed system. Recall the AO system is a direct measurement of the transverse velocity, while the other systems contain upshifted heterodyne signals which observe components longitudinal and transverse velocity.

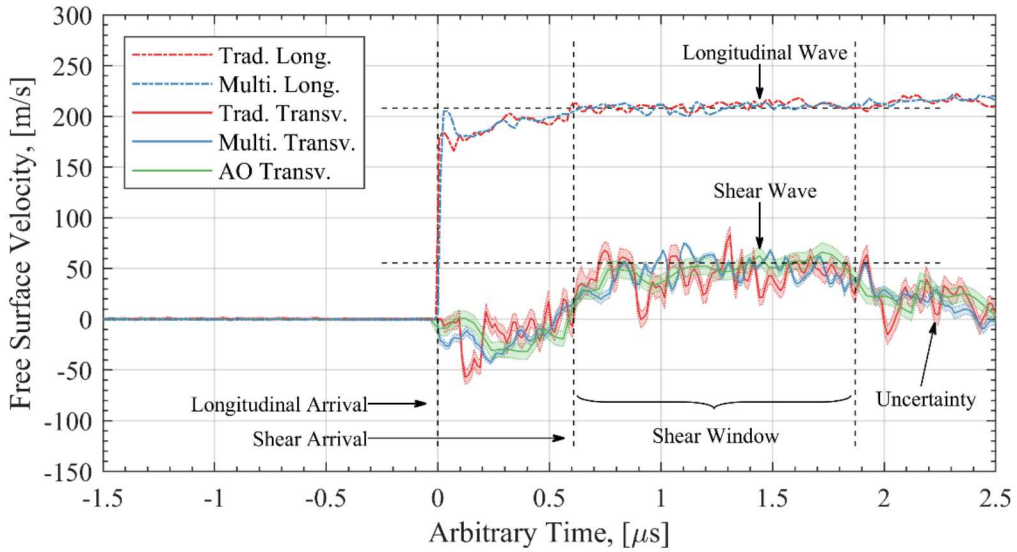

FIGURE 4. Overlay of the resolved PDV traces. Longitudinal velocities are illustrated for both heterodyne techniques. Transverse velocities are illustrated for the three systems and have uncertainty illustrated by bounds. Vertical lines illustrate the expected longitudinal and shear wave arrival times, as well as the shear window in the experiment.

ACKNOWLEDGEMENTS

Sandia National Laboratories is a multimission laboratory managed and operated by National Technology & Engineering Solutions of Sandia, LLC, a wholly owned subsidiary of Honeywell International Inc., for the U.S. Department of Energy's National Nuclear Security Administration under contract DE-NA0003525.

REFERENCES

[1] O. T. Strand, L. V Berzins, D. R. Goosman, W. Kuhlow, P. D. Sargis, and T. L. Whitworth, "Velocimetry Using Heterodyne Techniques," 2004.

[2] O. T. Strand, D. R. Goosman, C. Martinez, T. L. Whitworth, and W. W. Kuhlow, “Compact system for high-speed velocimetry using heterodyne techniques,” *Rev. Sci. Instrum.*, vol. 77, no. 8, pp. 1–8, 2006.
[3] K. S. Kim, R. J. Clifton, and P. Kumar, “A combined normal- and transverse-displacement interferometer with an application to impact of y-cut quartz,” *J. Appl. Phys.*, vol. 48, no. 10, pp. 4132–4139, 1977.
[4] A. S. Abou-Sayed *et al.*, “The Oblique-plate Impact Experiment,” *Exp. Mech.*, vol. 16, no. 4, pp. 127–132, Apr. 1976.
[5] A. S. Abou-Sayed and R. J. Clifton, “Pressure shear waves in fused silica,” vol. 47, no. 1762, 1976.
[6] K. J. Frutschy and R. J. Clifton, “High-temperature Pressure-shear Plate Impact Experiments Using Pure Tungsten Carbide Impactors,” vol. 38, no. 2, 1998.
[7] R. W. Klopp, R. J. Clifton, and T. G. Shawki, “Pressure-shear impact and the dynamic viscoplastic response of metals,” *Mech. Mater.*, vol. 4, no. 3–4, pp. 375–385, 1985.
[8] S. Sundaram, “Pressure-Shear Plate Impact Studies of Alumina Ceramics and the Influence of an Intergranular Glassy Phase,” Brown University, 1998.
[9] T. J. Vogler, C. S. Alexander, T. F. Thornhill, and W. D. Reinhart, “Pressure-Shear Experiments on Granular Materials,” Albuquerque, New Mexico, 2011.
[10] K. J. Frutschy, “High-Temperature Pressure-Shear Plate Impact Experiments on OFHC Copper and Pure Tungsten Carbide,” Brown University, 1992.
[11] J. W. Lajeunesse, “Dynamic Behavior of Granular Earth Materials Subjected to Pressure-Shear Loading,” Marquette University, 2018.
[12] P. A. Sable, “Multi-Scale Traction Dynamics in Obliquely Impacted Polymer-Metal Targets,” Marquette University, 2019.
[13] W. Tong, “Pressure-Shear Impact Investigation of Strain-Rate History Effects in OFHC Copper,” Brown University, 1991.
[14] A. Gilat and R. J. Clifton, “PRESSURE-SHEAR WAVES IN 6061-T6 ALUMINUM,” *J. Mech. Physi. Solids*, vol. 33, no. 3, pp. 263–284, 1985.
[15] K. T. Ramesh and R. J. Clifton, “A Pressure-Shear Plate Impact Experiment for Studying the Rheology of Lubricants at High Pressures and High Shearing Rates,” *J. Tribol.*, vol. 109, no. 2, pp. 215–222, 1987.
[16] R. J. Clifton and S. Huang, “PRESSURE-SHEAR IMPACT INVESTIGATION OF STRAIN RATE HISTORY EFFECTS IN OXYGEN-FREE,” vol. 40, no. 6, 1992.
[17] K. S. Kim, “Pressure-Shear Impact of 6061-T6,” vol. 4, no. 79, 2019.
[18] B. Zuanetti, T. Wang, and V. Prakash, “A compact fiber optics-based heterodyne combined normal and transverse displacement interferometer,” *Rev. Sci. Instrum.*, vol. 88, no. 3, pp. 1–7, 2017.
[19] C. Kettenbeil, M. Mello, M. Bischann, and G. Ravichandran, “Heterodyne transverse velocimetry for pressure-shear plate impact experiments,” *J. Appl. Phys.*, vol. 123, no. 12, pp. 1–14, 2018.
[20] D. H. Dolan, M. Elert, M. D. Furnish, W. W. Anderson, W. G. Proud, and W. T. Butler, “WHAT DOES ‘VELOCITY’ INTERFEROMETRY REALLY MEASURE?,” in *AIP Conference Proceedings*, 2009, pp. 589–594.
[21] G. Chen, D. Wang, J. Liu, J. Meng, S. Liu, and Q. Yang, “A novel photonic Doppler velocimetry for transverse velocity measurement,” *Rev. Sci. Instrum.*, vol. 84, no. 1, 2013.
[22] C. R. Johnson, J. W. Lajeunesse, P. A. Sable, A. Dawson, A. Hatzenbihler, and J. P. Borg, “Photon Doppler velocimetry measurements of transverse surface velocities,” *Rev. Sci. Instrum.*, vol. 89, no. 6, 2018.
[23] E. Daykin *et al.*, “Multiplexed photonic Doppler velocimetry for large channel count experiments Multiplexed Photonic Doppler Velocimetry for Large Channel Count Experiments,” vol. 160004, no. January, 2017.
[24] E. A. Moro, “New Developments in Photon Doppler Velocimetry,” *APS-SCCM Conf. Proc.*, 2013.
[25] J. R. Danielson, “Measurement of an explosively driven hemispherical shell using 96 points of optical velocimetry,” *J. Phys.*, vol. 500, 2014.
[26] T. Ao and D. H. Dolan, “SIRHEN : a data reduction program for photonic Doppler velocimetry measurements,” no. June, 2010.
[27] D. H. Dolan, T. Ao, and S. C. Grant, “The Sandia Matlab AnalysiS Hierarchy (SMASH) toolbox,” no. August, 2016.
[28] D. H. Dolan, “Accuracy and precision in photonic doppler velocimetry,” *Rev. Sci. Instrum.*, vol. 81, no. 5, 2010.